Comparative Analysis of Specular and Diffuse Reflection Near-Infrared Spectra in Wood Species Classification

Cheng-Kun Wang, a Peng Zhao, b,c,* Li-Na Dong, a and Mao-Ni Zhao a

The near-infrared (NIR) spectral reflectance characteristics of wood cross sections are commonly employed for wood species classification. Both specular and diffuse reflectance spectral curves of wood cross sections can be used. However, which one is more effective for classification and whether classification models trained on these two spectra can be used interchangeably have not yet been explored. In this study, the NIR spectral curves of wood cross sections from 64 common timber species were used to evaluate the specular and diffuse reflectance spectral profiles through five classifier models—namely, the support vector machine (SVM), knearest neighbors (KNN), convolutional neural network (CNN), decision tree (DT), and nearest class mean (NCM) classifiers. The classification accuracies of specular and diffuse reflectance curves using SVM classifier were 88.43% and 88.02%, respectively, whereas other classifiers exhibited lower classification accuracy, with specular reflectance spectral classification accuracy consistently outperforming diffuse spectral classification. Additionally, experimental results demonstrated that correct classification rate of the testing dataset after cross-use was less than 16%, indicating that classifier models trained on these two spectra could not be used interchangeably. In conclusion, this study suggested that specular reflectance NIR spectral curves are more suitable for wood species classification.

DOI: 10.15376/biores.20.3.6648-6661

Keywords: Wood species classification; Specular reflectance spectrum; Diffuse reflectance spectrum; Spectral analysis

Contact information: a: School of Electronic and Information Engineering, Heilongjiang University of Science and Technology, Harbin 150010, China; b: School of Computer Science and Communication Engineering, Guangxi University of Science and Technology, Liuzhou 545006, China; c: Guangxi Colleges and Universities Key Laboratory of Intelligent Computing and Distributed Information Processing, Liuzhou 545006, China. *Corresponding author: bit_zhao@aliyun.com

INTRODUCTION

There are an estimated 60,065 timber species worldwide. Currently, five main methods are used to identify them, namely image processing classification (Verly Lopes *et al.* 2020), spectral analysis classification (Ma *et al.* 2019), wood microstructure classification (Zhan *et al.* 2023), deoxyribonucleic acid (DNA) genetic information classification (Antil *et al.* 2023), and chemical fingerprinting classification (Deklerck *et al.* 2020). Among these methods, spectral analysis classification offers advantages that include its high classification speed, high accuracy, and low computational overhead. Spectral analysis itself can be further divided into four distinct categories. The first category involves Fourier transform infrared (FTIR) analysis for wood species classification, which

is a rapid, nondestructive method (Sharma et al. 2020). However, it requires sophisticated equipment and stringent experimental conditions. The second category employs terahertz spectroscopy to identify wood species. For example, Zhang et al. (2023) used terahertz time-domain spectroscopy to classify wood species by measuring the spectral differences of manglietia, amur linden, black walnut, and ebony in the 0.1 to 0.9 THz frequency range in combination with principal component analysis. However, high-quality terahertz equipment can be expensive and requires precise sample preparation. The third category leverages hyperspectral imaging by combining the spectral and image information from wood surfaces for classification. Kanayama et al. (2019) used hyperspectral images and a convolutional neural network (CNN) model to classify wood species. However, hyperspectral imaging devices can be costly and the process of collecting hyperspectral images from wood surfaces can be time-consuming, resulting in poor real-time performance.

In summary, these three methods rely on expensive instrumentation and are generally more suitable for laboratory-based testing and processing. The fourth category involves the use of a cheap micro-spectrometer to collect spectral reflectance curves from wood cross sections for classification. The cheap micro-spectrometers employed in this method are generally more affordable and well-suited for on-site inspection and processing. For example, Luo et al. (2023) used near-infrared (NIR) spectroscopy in combination with six classifier models—that is, that support vector machine (SVM), logistic regression, Naïve Bayes, k-nearest neighbors (KNN), random forest, and artificial neural network models—to classify 12 timber species. The experimental results demonstrated that the SVM-based model achieved the highest classification accuracy (98.24%). Wang et al. (2024) investigated the deformation of the corresponding NIR spectral curves and their correction after applying a transparent finish to the wood surfaces, before using the corrected NIR spectral curves to classify and recognize the wood species, achieving high classification accuracy. During the collection of NIR spectral reflectance curves using the miniature spectrometer, variations in the incident angles of the fiber-optic probe relative to the object's surface can result in two types of spectra: specular reflectance and diffuse reflectance. The corresponding spectral reflectance curves exhibit distinct differences. However, the question of which spectral reflectance curve provides better classification and recognition accuracy, and whether classifier models trained on these two distinct spectral profiles can be used interchangeably, has not yet been addressed.

Consequently, this study focused on 64 common wood species to compare and investigate the use of specular and diffuse reflectance spectra from wood cross sections for species classification and recognition. It further analyzed the classification accuracy of wood species in both cases and explored the potential for cross-using classifier models trained on them both.

EXPERIMENTAL

Materials

In this study, 64 hardwood and coniferous wood species were used as the experimental subjects. The specific details of these wood species are provided in Table 1, which demonstrates that they included both species from the same genus and those with visually similar textures. The spectral reflectance profiles of the wood sample cross sections were collected using a micro-spectrometer. Timber samples were prepared

following national standards. For each species, 25 pieces of sawn timber pieces from different trees at different locations were selected. These pieces were uniformly cut into small blocks measuring $2 \times 2 \times 3$ cm³, with the 2×2 cm² side representing the cross section and the 2×3 cm² side representing either the tangential or radial section. From the cut pieces, 50 small blocks were randomly selected as experimental samples for data collection, with two blocks being selected from each sawn timber sample. Prior to spectral data collection, the cross sections of the wood samples were sanded individually using 800-grit and 1200-grit sandpaper to ensure that the surfaces were smooth and free of burrs.

In practice, the wood NIR spectral curves may be sensitive to some external environmental factors, such as temperature and humidity, so the spectral acquisition was performed in a room with temperature at 25 °C and humidity at 40%. It should be noted that the physical property of wood samples was influenced by some variables such as the age of trees, geographic origin, growth ring position, and proportion of latewood versus earlywood. These variables were controlled effectively in wood spectral acquisition so that the within-class difference of spectral curves for each wood species was adequately small. This control was implemented in practice in the random selection of 50 wood blocks for every wood species by ensuring that $trace(C_w)$ was small or less than a threshold for every species (i.e., Cw denoted the within-class scatter matrix for one class in terms of spectral curves). Specifically, in the spectral acquisition process, spectral curves were collected from five different positions on the cross section of one wood sample block, and the mean spectral curve was saved as the final curve. This was done to decrease the within-class difference of spectral curves for each wood species to some extent. Every selected wood block was used in spectral acquisition for both specular and diffuse reflection spectral curves to ensure the subsequent objective comparisons.

 Table 1. Detailed Information on the Wood Species Samples

Number	Genus	Species
1	Acer	davidii
2	Amygdalus	davidiana
3	Aucoumea	klaineana
4	Betula	alnoides
5	Betula	platyphylla
6	Calophyllum	inophyllum
7	Chamaecyparis	nootkatensis
8	Cinnamomum	camphora
9	Cyclobalanopsis	glauca
10	Dipterocarpus	alatus
11	Entandrophragma	candollei
12	Fraxinus	chinensis
13	Fraxinus	mandshurica
14	Guibourtia	demeusei
15	Guibourtia	ehie
16	Intsia	bijuga
17	Juglans	mandshurica
18	Juglans	nigra
19	Larix	gmelinii
20	Magnolia	fordiana
21	Millettia	laurentii
22	Picea	asperata
23	Pinups	radiata
24	Pinups	koraiensis

26 Pinups sylvestris 27 Platanus orientalis 28 Pometia pinnata 29 Populus alba 30 Populus tomentosa 31 Populus sylvestria 32 Pouteria speciosa 33 Prunus avium 34 Pseudotsuga menziesii 35 Pterocarpus soyauxii 36 Quercus mongolica 37 Quercus acutissima 38 Rhodamnia dumetorum 39 Robinia pseudoacacia 40 Salix matsudana 41 Shorea contorta 42 Shorea laevis 43 Sophora japonica 44 Swietenia mahagoni 45 Tectona grandis 46 Terminalia cattapa 47 Tilla mandshurica 48 Toona cillata 49 Ulmus glabra 50 Vernicia fordii 51 Pterocarpus marcocarpus 55 Pterocarpus marcocarpus 56 Distemonanthus benthaminanus 57 Cylicodiscus gabunensis 58 Albizia kalkora 59 Berlinia confusa 60 Daniellia oliveri 61 Sabina chinensis 62 Acer pictum 61 Hovenia dulcis	25	Pinups	massoniana		
27 Platanus orientalis 28 Pometia pinnata 29 Populus alba 30 Populus cathayana 31 Populus tomentosa 32 Pouteria speciosa 33 Prunus avium 34 Pseudotsuga menziesii 35 Pterocarpus soyauxii 36 Quercus mongolica 37 Quercus acutissima 38 Rhodamnia dumetorum 39 Robinia pseudoacacia 40 Sailix matsudana 41 Shorea contorta 42 Shorea laevis 43 Sophora japonica 444 Swietenia mahagoni 45 Tectona grandis 46 Terminalia cattapa 47 Tillia mandshurica 48 Toona ciliata 49 Ulmus glabra 50 Vernicia fordii 51 Pterocarpus macrocarpus 51 Pterocarpus macrocarpus 52 Pterocarpus erinaceus 53 Pterocarpus macrocarpus 54 Pterocarpus macrocarpus 55 Cryptomeria fortune 56 Distemonanthus benthaminanus 57 Cylicodiscus gabunensis 58 Albizia kalkora 59 Berlinia confusa 60 Daniellia oliveri 61 Sabina chinensis 62 Acer pictum					
28 Pometia pinnata 29 Populus alba 30 Populus cathayana 31 Populus tomentosa 32 Pouteria speciosa 33 Prunus avium 34 Pseudotsuga menziesii 35 Pterocarpus soyauxii 36 Quercus mongolica 37 Quercus acutissima 38 Rhodamnia dumetorum 39 Robinia pseudoacacia 40 Sailx matsudana 41 Shorea contorta 42 Shorea laevis 43 Sophora japonica 44 Swietenia mahagoni 45 Tectona grandis 46 Terminalia cattapa 47 Tilia mandshurica 48 Toona ciliata 49 Ulmus glabra 50 Vernicia fordii 51 Pterocarpus macrocarpus macrocarpus 52 Pterocarpus macrocarpus macrocarpus 53 Pterolaina pseudoacacia 59 Berlinia confusa 50 Distemonanthus benthaminanus 57 Cylicodiscus gabunensis 58 Albizia kalkora 59 Berlinia confusa 60 Daniellia oliveri 61 Sabina chinensis 62 Acer pictum		,			
29 Populus alba 30 Populus cathayana 31 Populus tomentosa 32 Pouteria speciosa 33 Prunus avium 34 Pseudotsuga menziesii 35 Pterocarpus soyauxii 36 Quercus mongolica 37 Quercus acutissima 38 Rhodamnia dumetorum 39 Robinia pseudoacacia 40 Salix matsudana 41 Shorea contorta 42 Shorea laevis 43 Sophora japonica 44 Swietenia mahagoni 45 Tectona grandis 46 Terminalia cattapa 47 Tilia mandshurica 48 Toona ciliata 49 Ulmus glabra 50 Vernicia fordii 51 Pterocarpus					
30 Populus cathayana 31 Populus tomentosa 32 Pouteria speciosa 33 Prunus avium 34 Pseudotsuga menziesii 35 Pterocarpus soyauxii 36 Quercus mongolica 37 Quercus acutissima 38 Rhodamnia dumetorum 39 Robinia pseudoacacia 40 Salix matsudana 41 Shorea contorta 42 Shorea laevis 43 Sophora japonica 44 Swietenia mahagoni 45 Tectona grandis 46 Terminalia cattapa 47 Tilia mandshurica 48 Toona ciliata 49 Ulmus glabra 50 Vemicia fordii 51 Pterocarpus antunesii 52 Pterocarpus macrocarpus 54 Pterocarpus erinaceus 55 Cryptomeria fortune 56 Distemonanthus benthaminanus 57 Cylicodiscus gabunensis 58 Albizia kalkora 60 Daniellia oliveri 61 Sabina chinensis 62 Acer pletocarpus amurense					
31 Populus tomentosa 32 Pouteria speciosa 33 Prunus avium 34 Pseudotsuga menziesii 35 Pterocarpus soyauxii 36 Quercus mongolica 37 Quercus acutissima 38 Rhodannia dumetorum 39 Robinia pseudoacacia 40 Sailx matsudana 41 Shorea contorta 42 Shorea laevis 43 Sophora japonica 44 Swietenia mahagoni 45 Tectona grandis 46 Terminalia cattapa 47 Tilia mandshurica 48 Toona ciliata 49 Ulmus glabra 50 Vernicia fordii 51 Pterocarpus antunesii 52 Pterocarpus macrocarpus 54 Pte					
32 Pouteria speciosa 33 Prunus avium 34 Pseudotsuga menziesii 35 Pterocarpus soyauxii 36 Quercus mongolica 37 Quercus acutissima 38 Rhodamnia dumetorum 39 Robinia pseudoacacia 40 Saiix matsudana 41 Shorea contorta 42 Shorea laevis 43 Sophora japonica 44 Swietenia mahagoni 45 Tectona grandis 46 Terminalia cattapa 47 Tilia mandshurica 48 Toona ciliata 49 Ulmus glabra 50 Vernicia fordii 51 Pterocarpus antunesii 52 Pterocarpus macrocarpus 53 Pterocarpus tinctorius 54 Pterocarpus gabunensis 55 Cryptomeria fortune 56 Distemonanthus benthaminanus 57 Cylicodiscus gabunensis 58 Albizia kalkora 59 Berlinia chire.					
33 Prunus avium 34 Pseudotsuga menziesii 35 Pterocarpus soyauxii 36 Quercus mongolica 37 Quercus acutissima 38 Rhodamnia dumetorum 39 Robinia pseudoacacia 40 Sailx matsudana 41 Shorea contorta 42 Shorea laevis 43 Sophora japonica 44 Swietenia mahagoni 45 Tectona grandis 46 Terminalia cattapa 47 Tilia mandshurica 48 Toona ciliata 49 Ulmus glabra 50 Vernicia fordii 51 Pterocarpus antunesii 52 Pterocarpus erinaceus 53 Pterocarpus macrocarpus 54 Pterocarpus fortune 55 Cryptomeria fortune 56 Distemonanthus benthaminanus 57 Cylicodiscus gabunensis 58 Albizia kalkora 60 Daniellia cliume 61 Sabina chinensis 62 Acer pictum 63 Phellodendron amurense					
34 Pseudotsuga menziesii 35 Pterocarpus soyauxii 36 Quercus mongolica 37 Quercus acutissima 38 Rhodamnia dumetorum 39 Robinia pseudoacacia 40 Sailx matsudana 41 Shorea contorta 42 Shorea laevis 43 Sophora japonica 44 Swietenia mahagoni 45 Tectona grandis 46 Terminalia cattapa 47 Tillia mandshurica 48 Toona ciliata 49 Ulmus glabra 50 Vernicia fordii 51 Pterocarpus antunesii 52 Pterocarpus erinaceus 53 Pterocarpus macrocarpus 54 Pterocarpus fortune 55 Cryptomeria fortune 56 Distemonanthus benthaminanus 57 Cylicodiscus gabunensis 58 Albizia kalkora 60 Daniellia chiera					
35 Pterocarpus soyauxii 36 Quercus mongolica 37 Quercus acutissima 38 Rhodamnia dumetorum 39 Robinia pseudoacacia 40 Saiix matsudana 41 Shorea contorta 42 Shorea laevis 43 Sophora japonica 444 Swietenia mahagoni 45 Tectona grandis 46 Terminalia cattapa 47 Tilia mandshurica 48 Toona ciliata 49 Ulmus glabra 50 Vernicia fordii 51 Pterocarpus antunesii 52 Pterocarpus macrocarpus 53 Pterocarpus macrocarpus 54 Pterocarpus fortune 56 Distemonanthus benthaminanus 57 Cylicodiscus gabunensis 58 Albizia kalkora 59 Berlinia chimensis 60 Acer pictum 61 Sabina chinensis 62 Acer					
36 Quercus mongolica 37 Quercus acutissima 38 Rhodamnia dumetorum 39 Robinia pseudocacia 40 Sailx matsudana 41 Shorea contorta 42 Shorea laevis 43 Sophora japonica 44 Swietenia mahagoni 45 Tectona grandis 46 Terminalia cattapa 47 Tilia mandshurica 48 Toona ciliata 49 Ulmus glabra 50 Vernicia fordii 51 Pterocarpus antunesii 52 Pterocarpus erinaceus 53 Pterocarpus tinctorius 55 Cryptomeria fortune 56 Distemonanthus benthaminanus 57 Cylicodiscus gabuneasis 58 Albizia kalkora 59 Berlinia chinensis 60 Acer pictum 61 Sabina chinensis 62 Acer pictum					
37 Quercus acutissima 38 Rhodamnia dumetorum 39 Robinia pseudoacacia 40 Sailx matsudana 41 Shorea contorta 42 Shorea laevis 43 Sophora japonica 44 Swietenia mahagoni 45 Tectona grandis 46 Terminalia cattapa 47 Tilia mandshurica 48 Toona ciliata 49 Ulmus glabra 50 Vernicia fordii 51 Pterocarpus antunesii 52 Pterocarpus erinaceus 53 Pterocarpus tinctorius 54 Pterocarpus gabunensis 55 Cryptomeria fortune 56 Distemonanthus benthaminanus 57 Cylicodiscus gabunensis 58 Albizia kalkora 59 Berlinia chinesis 60 Acer pictum 61 Sabina chinensis 62 Acer pictum 63 Phellodendron amurense					
38Rhodamniadumetorum39Robiniapseudoacacia40Sailxmatsudana41Shoreacontorta42Shorealaevis43Sophorajaponica44Swieteniamahagoni45Tectonagrandis46Terminaliacattapa47Tiliamandshurica48Toonaciliata49Ulmusglabra50Verniciafordii51Pterocarpusantunesii52Pterocarpuserinaceus53Pterocarpusmacrocarpus54Pterocarpustinctorius55Cryptomeriafortune56Distemonanthusbenthaminanus57Cylicodiscusgabunensis58Albiziakalkora59Berliniaconfusa60Danielliaoliveri61Sabinachinensis62Acerpictum63Phellodendronamurense					
39 Robinia pseudoacacia 40 Sailx matsudana 41 Shorea contorta 42 Shorea laevis 43 Sophora japonica 44 Swietenia mahagoni 45 Tectona grandis 46 Terminalia cattapa 47 Tilia mandshurica 48 Toona ciliata 49 Ulmus glabra 50 Vernicia fordii 51 Pterocarpus antunesii 52 Pterocarpus erinaceus 53 Pterocarpus macrocarpus 54 Pterocarpus tinctorius 55 Cryptomeria fortune 56 Distemonanthus benthaminanus 57 Cylicodiscus gabunensis 58 Albizia kalkora 59 Berlinia confusa 60 Daniellia oliveri 61<					
40 Sailx matsudana 41 Shorea contorta 42 Shorea laevis 43 Sophora japonica 44 Swietenia mahagoni 45 Tectona grandis 46 Terminalia cattapa 47 Tilia mandshurica 48 Toona ciliata 49 Ulmus glabra 50 Vernicia fordii 51 Pterocarpus antunesii 52 Pterocarpus erinaceus 53 Pterocarpus macrocarpus 54 Pterocarpus tinctorius 55 Cryptomeria fortune 56 Distemonanthus benthaminanus 57 Cylicodiscus gabunensis 58 Albizia kalkora 59 Berlinia confusa 60 Daniellia oliveri 61 Sabina chinensis 62					
41 Shorea contorta 42 Shorea laevis 43 Sophora japonica 44 Swietenia mahagoni 45 Tectona grandis 46 Terminalia cattapa 47 Tilia mandshurica 48 Toona ciliata 49 Ulmus glabra 50 Vernicia fordii 51 Pterocarpus antunesii 52 Pterocarpus erinaceus 53 Pterocarpus macrocarpus 54 Pterocarpus tinctorius 55 Cryptomeria fortune 56 Distemonanthus benthaminanus 57 Cylicodiscus gabunensis 58 Albizia kalkora 59 Berlinia confusa 60 Daniellia oliveri 61 Sabina chinensis 62 Acer pictum 63			· ·		
42 Shorea laevis 43 Sophora japonica 44 Swietenia mahagoni 45 Tectona grandis 46 Terminalia cattapa 47 Tilia mandshurica 48 Toona ciliata 49 Ulmus glabra 50 Vernicia fordii 51 Pterocarpus antunesii 52 Pterocarpus erinaceus 53 Pterocarpus macrocarpus 54 Pterocarpus tinctorius 55 Cryptomeria fortune 56 Distemonanthus benthaminanus 57 Cylicodiscus gabunensis 58 Albizia kalkora 59 Berlinia confusa 60 Daniellia oliveri 61 Sabina chinensis 62 Acer pictum 63 Phellodendron amurense					
43 Sophora japonica 44 Swietenia mahagoni 45 Tectona grandis 46 Terminalia cattapa 47 Tilia mandshurica 48 Toona ciliata 49 Ulmus glabra 50 Vernicia fordii 51 Pterocarpus antunesii 52 Pterocarpus erinaceus 53 Pterocarpus macrocarpus 54 Pterocarpus tinctorius 55 Cryptomeria fortune 56 Distemonanthus benthaminanus 57 Cylicodiscus gabunensis 58 Albizia kalkora 59 Berlinia confusa 60 Daniellia oliveri 61 Sabina chinensis 62 Acer pictum 63 Phellodendron amurense					
44 Swietenia mahagoni 45 Tectona grandis 46 Terminalia cattapa 47 Tilia mandshurica 48 Toona ciliata 49 Ulmus glabra 50 Vernicia fordii 51 Pterocarpus antunesii 52 Pterocarpus erinaceus 53 Pterocarpus macrocarpus 54 Pterocarpus tinctorius 55 Cryptomeria fortune 56 Distemonanthus benthaminanus 57 Cylicodiscus gabunensis 58 Albizia kalkora 59 Berlinia confusa 60 Daniellia oliveri 61 Sabina chinensis 62 Acer pictum 63 Phellodendron amurense			laevis		
45Tectonagrandis46Terminaliacattapa47Tiliamandshurica48Toonaciliata49Ulmusglabra50Verniciafordii51Pterocarpusantunesii52Pterocarpuserinaceus53Pterocarpusmacrocarpus54Pterocarpustinctorius55Cryptomeriafortune56Distemonanthusbenthaminanus57Cylicodiscusgabunensis58Albiziakalkora59Berliniaconfusa60Danielliaoliveri61Sabinachinensis62Acerpictum63Phellodendronamurense			japonica		
46TerminaliaCattapa47Tiliamandshurica48Toonaciliata49Ulmusglabra50Verniciafordii51Pterocarpusantunesii52Pterocarpuserinaceus53Pterocarpusmacrocarpus54Pterocarpustinctorius55Cryptomeriafortune56Distemonanthusbenthaminanus57Cylicodiscusgabunensis58Albiziakalkora59Berliniaconfusa60Danielliaoliveri61Sabinachinensis62Acerpictum63Phellodendronamurense		Swietenia	mahagoni		
47Tiliamandshurica48Toonaciliata49Ulmusglabra50Verniciafordii51Pterocarpusantunesii52Pterocarpuserinaceus53Pterocarpusmacrocarpus54Pterocarpustinctorius55Cryptomeriafortune56Distemonanthusbenthaminanus57Cylicodiscusgabunensis58Albiziakalkora59Berliniaconfusa60Danielliaoliveri61Sabinachinensis62Acerpictum63Phellodendronamurense			grandis		
48 Toona ciliata 49 Ulmus glabra 50 Vernicia fordii 51 Pterocarpus antunesii 52 Pterocarpus erinaceus 53 Pterocarpus macrocarpus 54 Pterocarpus tinctorius 55 Cryptomeria fortune 56 Distemonanthus benthaminanus 57 Cylicodiscus gabunensis 58 Albizia kalkora 59 Berlinia confusa 60 Daniellia oliveri 61 Sabina chinensis 62 Acer pictum 63 Phellodendron amurense					
49Ulmusglabra50Verniciafordii51Pterocarpusantunesii52Pterocarpuserinaceus53Pterocarpusmacrocarpus54Pterocarpustinctorius55Cryptomeriafortune56Distemonanthusbenthaminanus57Cylicodiscusgabunensis58Albiziakalkora59Berliniaconfusa60Danielliaoliveri61Sabinachinensis62Acerpictum63Phellodendronamurense		Tilia	mandshurica		
50Verniciafordii51Pterocarpusantunesii52Pterocarpuserinaceus53Pterocarpusmacrocarpus54Pterocarpustinctorius55Cryptomeriafortune56Distemonanthusbenthaminanus57Cylicodiscusgabunensis58Albiziakalkora59Berliniaconfusa60Danielliaoliveri61Sabinachinensis62Acerpictum63Phellodendronamurense		Toona	ciliata		
51Pterocarpusantunesii52Pterocarpuserinaceus53Pterocarpusmacrocarpus54Pterocarpustinctorius55Cryptomeriafortune56Distemonanthusbenthaminanus57Cylicodiscusgabunensis58Albiziakalkora59Berliniaconfusa60Danielliaoliveri61Sabinachinensis62Acerpictum63Phellodendronamurense	49	Ulmus	glabra		
52 Pterocarpus erinaceus 53 Pterocarpus macrocarpus 54 Pterocarpus tinctorius 55 Cryptomeria fortune 56 Distemonanthus benthaminanus 57 Cylicodiscus gabunensis 58 Albizia kalkora 59 Berlinia confusa 60 Daniellia oliveri 61 Sabina chinensis 62 Acer pictum 63 Phellodendron amurense	50	Vernicia	fordii		
53 Pterocarpus macrocarpus 54 Pterocarpus tinctorius 55 Cryptomeria fortune 56 Distemonanthus benthaminanus 57 Cylicodiscus gabunensis 58 Albizia kalkora 59 Berlinia confusa 60 Daniellia oliveri 61 Sabina chinensis 62 Acer pictum 63 Phellodendron amurense	51	Pterocarpus	antunesii		
54Pterocarpustinctorius55Cryptomeriafortune56Distemonanthusbenthaminanus57Cylicodiscusgabunensis58Albiziakalkora59Berliniaconfusa60Danielliaoliveri61Sabinachinensis62Acerpictum63Phellodendronamurense	52	Pterocarpus	erinaceus		
54 Pterocarpus tinctorius 55 Cryptomeria fortune 56 Distemonanthus benthaminanus 57 Cylicodiscus gabunensis 58 Albizia kalkora 59 Berlinia confusa 60 Daniellia oliveri 61 Sabina chinensis 62 Acer pictum 63 Phellodendron amurense		Pterocarpus	macrocarpus		
55 Cryptomeria fortune 56 Distemonanthus benthaminanus 57 Cylicodiscus gabunensis 58 Albizia kalkora 59 Berlinia confusa 60 Daniellia oliveri 61 Sabina chinensis 62 Acer pictum 63 Phellodendron amurense			tinctorius		
57Cylicodiscusgabunensis58Albiziakalkora59Berliniaconfusa60Danielliaoliveri61Sabinachinensis62Acerpictum63Phellodendronamurense	55	Cryptomeria	fortune		
57Cylicodiscusgabunensis58Albiziakalkora59Berliniaconfusa60Danielliaoliveri61Sabinachinensis62Acerpictum63Phellodendronamurense	56	Distemonanthus	benthaminanus		
58Albiziakalkora59Berliniaconfusa60Danielliaoliveri61Sabinachinensis62Acerpictum63Phellodendronamurense					
59Berliniaconfusa60Danielliaoliveri61Sabinachinensis62Acerpictum63Phellodendronamurense	58				
60 Daniellia oliveri 61 Sabina chinensis 62 Acer pictum 63 Phellodendron amurense	59	Berlinia	confusa		
61 Sabina chinensis 62 Acer pictum 63 Phellodendron amurense		Daniellia			
62 Acer pictum 63 Phellodendron amurense	61				
63 Phellodendron amurense					
			•		

A Flame-NIR mini-spectrometer (Ocean Optics, Orlando, FL, USA), which offers advantages, such as portability, high accuracy, and rapid acquisition, was used in this study. Its operating range was 950 to 1650 nm; the NIR spectrum within this range provides greater stability compared to the visible light spectra. To ensure spectral accuracy, both the indoor temperature and light conditions were stabilized during spectrum collection. The environment for spectrum acquisition in this study was maintained at 25 °C and 40% relative humidity. The spectral data acquisition platform used in the experiment is illustrated in (Fig. 1), where ① is the sample under test, ② is the spectral reflectance acquisition kit, ③ is the cold light source, ④ is the computer, ⑤ is the Flame-NIR spectrometer, and ⑥ is the calibration plate.

The spectral reflectance collection process proceeded as follows. First, the equipment and light source were powered on and allowed to run for a period to ensure

system stabilization. The integration time was set to auto-mode, and calibration was performed using black and white calibration plates. Following calibration, a wood sample was placed at the designated position, and the spectral data were collected. Because the spectral reflectance of the wood sample correlated with the location of data collection, slight differences in spectral reflectance were evident when the fiber-optic probe was positioned at different points on the wood cross section. Consequently, during the spectral acquisition process, spectral data were collected from five different positions on the wood sample and the mean spectral curve was saved as the final curve to decrease the within-class difference of spectral curves for each wood species to some extent. Additionally, calibration was performed for every 20 samples to ensure the accuracy of the spectral data.



Fig. 1. Near-infrared spectral data acquisition platform for the wood samples

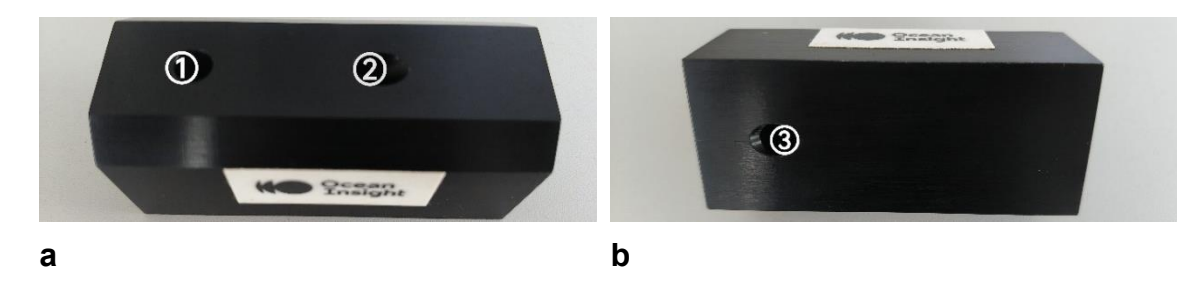


Fig. 2. Spectral reflectance acquisition kit: a. Front view of the kit; b. Back view of the kit

In the process of collecting spectral data, the specular reflectance and diffuse reflectance spectra of the wood cross section were collected separately, and a spectral reflectance acquisition kit from Ocean Optics was assembled, as illustrated in (Fig. 2). The kit comprised a fixed stand with two openings facing upwards, marked as ① and ② in (Fig. 2a and Fig. 3a), which were internally connected. The back of the kit had one additional opening, as illustrated in (Fig. 2b and Fig. 3a). When inserting the optical fiber into ① (as shown in (Fig. 3a and Fig. 3b)), the optical fiber probe could vertically illuminate the surface of the wood, enabling the collection of the specular reflectance spectrum from the cross section of the sample. By inserting the optical fiber into ② (as shown in (Fig. 3a and Fig. 3c)), the optical fiber probe could be tilted at a 45° angle to irradiate the wood's surface, allowing for the capture of the diffuse reflectance spectrum from the cross section of the sample. As illustrated in (Fig. 3b and Fig. 3c), the specular and diffuse reflectance rays returned along the same way that the incident ray has just come along, respectively.

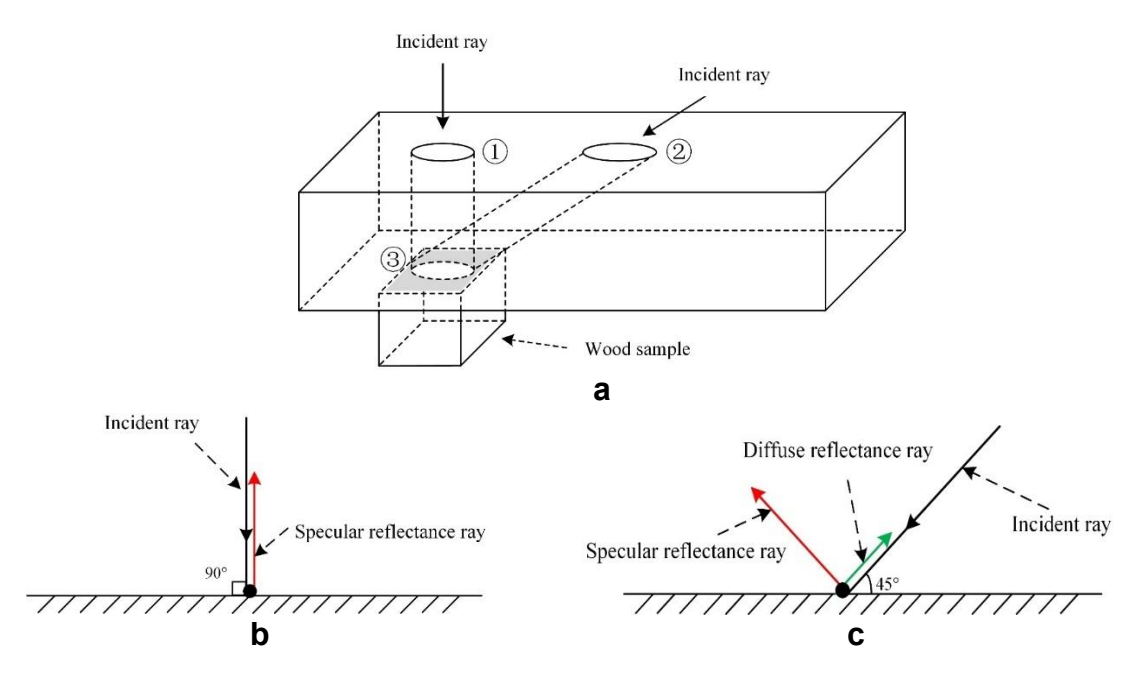


Fig. 3. Specular and diffuse reflectance spectral acquisition: a. Side view of the kit; b. Specular reflectance optical route; c. Diffuse reflectance optical route

Basic Process

The basic process used in this study is illustrated in Fig. 4. First, the specular and diffuse reflectance spectra for the wood samples listed in Table 1 were collected, and datasets were constructed for the wood sample cross sections.

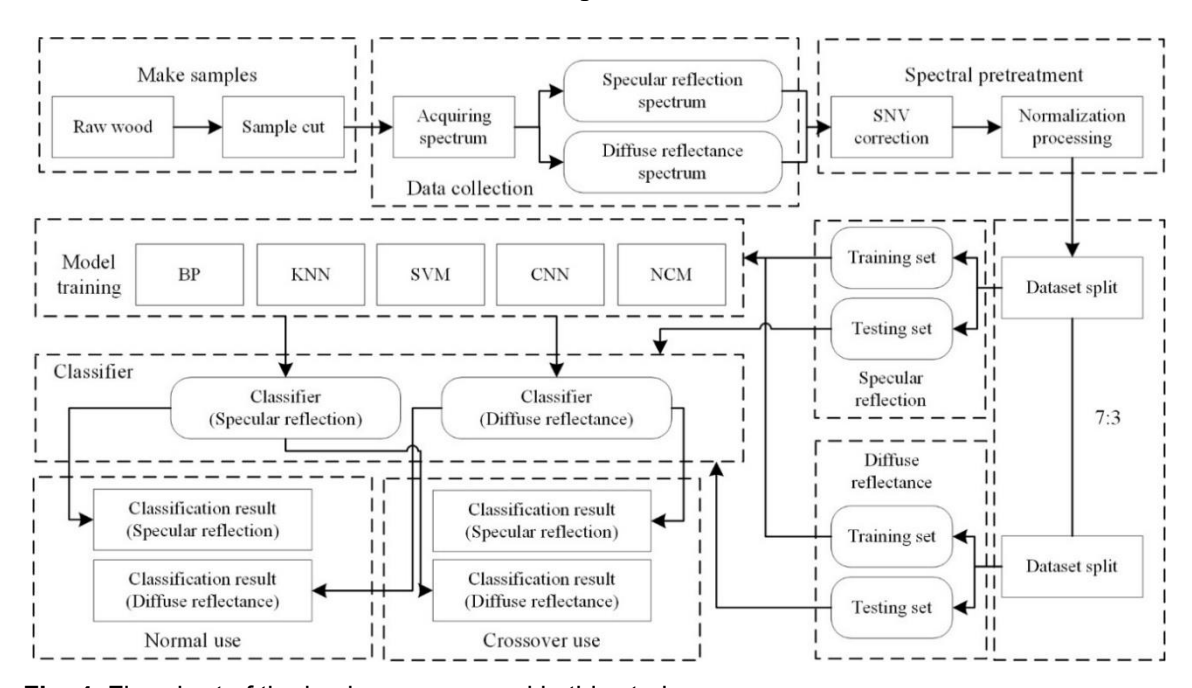


Fig. 4. Flowchart of the basic process used in this study

Spectral preprocessing was conducted first, including standard normal variate correction and normalization of the spectra using the min-max scaling method. To prevent overfitting, the dataset was randomly divided into training and test datasets in a 7:3 ratio.

Each wood species in the training dataset contained 35 samples, resulting in a training dataset size of 128×2240 , and each wood species in the test dataset contained 15 samples, resulting in a test dataset size of 128×960 . The NIR spectral vectors were 128-dimensional (128D). The SVM, KNN, CNN, decision tree (DT), and nearest class mean (NCM) classifiers were used to train and test the specular and diffuse reflection spectra. Next, a comparative analysis was conducted to examine the differences in classification accuracy between the specular and diffuse reflection spectra for wood species recognition. The possibility of cross-using classifier models trained on these two types of spectra was also explored.

It is important to note that the dataset was randomly divided each time training occurred; therefore, the classification accuracy of the trained classifier models varied across the test datasets. Consequently, for each classifier, the training and test datasets were randomly divided, trained, and tested 20 times, with the average classification accuracy being calculated.

Classifier Parameter Setting

The SVM is a supervised learning model used for classification and regression. It performs classification by finding a hyperplane that maximizes the distance between different categories (Hearst *et al.* 1998). In this study, a radial basis function was employed, with optimal parameters determined through a grid search method. To prevent overfitting, the classification accuracy was determined *via* cross-validation. The KNN model classifies samples by calculating the distance between the sample to be classified and all samples in the training dataset, identifying the k-nearest neighbors and then voting or performing weighted voting based on their labels (Peterson 2009). In this study, the Euclidean distance was used, with parameter k set to 3.

The CNNs typically comprise three parts—that is, a convolutional layer, a pooling layer, and a fully connected layer (Pan *et al.* 2023). The CNN structure used in this study comprised two convolutional layers, two pooling layers, one fully connected layer, and one output layer. Because the spectral reflectance of wood is one-dimensional, it must be processed using a one-dimensional convolution kernel. In contrast, 128D spectral vectors exhibit low dimensionality, leading the CNN to perform two rounds of convolution and pooling. Increasing the number of convolutions and pooling layers further reduces the dimensionality of the convolutional features to an excessively small scale. The specific parameters of the CNN used in this study were a one-dimensional convolution kernel of [–2,2,1] with valid convolution (without padding), and a pooling layer using the MaxPooling method. The original NIR spectrum was 128D, with the dimension reduced to 126D after the first convolution layer. The pooling step was set to 1, with a pooling width of 4, resulting in a dimensionality of 32D following the pooling operation. After further convolution and pooling, the final dimension was 8D.

The DT is a tree-structured supervised learning algorithm that classifies a dataset using a series of conditional judgments (Safavian and Landgrebe 1991). In this study, a fine tree was used, and the maximum number of splits was set at 100. The NCM classifier is a class-centered classification method that compares the distances between the sample to be classified and the class centers of all categories, assigning the sample to the closest class (Veenman and Reinders 2005).

RESULTS AND DISCUSSION

Comparison of Spectral Curves of Specular and Diffuse Reflections

The specular and diffuse reflectance spectra of the five wood cross sections are illustrated in Fig. 5. The spectral curves for the specular and diffuse reflections of the same wood species followed similar trends, with only slight shifts in their values. Additionally, the reflectance of the diffuse reflections was generally higher than that of the specular reflections. To quantitatively analyze the difference in mode separability information between the specular and diffuse reflectance spectra, three metrics based on scatter matrices were employed. These metrics can be defined as follows:

$$J_1 = \frac{tr(S_b)}{tr(S_w)'},\tag{1}$$

$$J_2 = tr(S_w^{-1}S_b), (2)$$

$$J_3 = |S_w^{-1} S_b| \tag{3}$$

where S_w denotes the total within-class scatter matrix for all classes, and S_b denotes the total between-class scatter matrix for all classes. Consequently, larger J_1 , J_2 , and J_3 , values resulted in better separability of the sample patterns.

Table 2 lists the three metrics calculated from the specular and diffuse reflectance spectra of the 64 wood species listed in Table 1. The specular reflectance spectra provided better pattern separability, suggesting that they should yield higher classification accuracy when applied to wood species classification and recognition.

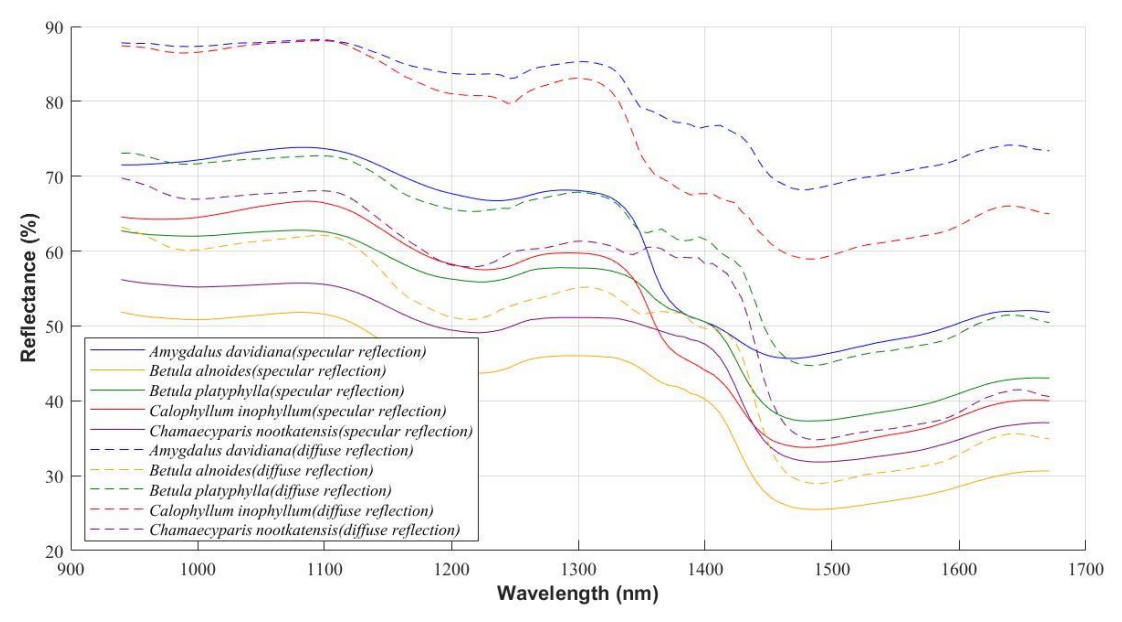


Fig. 5. Comparison of specular and diffuse spectral reflectance curves for cross sections of the same wood sample

Table 2. Comparison of Mode Separability Informativeness of Specular and Diffuse Reflectance Spectra

	J_1	J_2	J_3
Specular reflectance spectrum	52.19	11338	3.82×10^{-4}
Diffuse reflectance spectrum	12.23	1915	2.14×10^{-32}

Comparison of Specular and Diffuse Spectral Classification Accuracy

The average correct classification rates of the five classifiers after 20 training and testing sessions are listed in Table 3. The classification accuracies of the specular and diffuse reflectance spectra under the SVM classifier were essentially the same. For the other classifiers, the classification accuracy of the specular reflectance spectra was higher than that of the diffuse reflectance spectra, consistent with the three metrics J_1 , J_2 , and J_3 in Table 2. Figure 6 illustrates the classification accuracy of the SVM classifier over 20 training and testing sessions. The classification accuracies of specular and diffuse reflectance spectra were similar, though the accuracy of the diffuse reflectance spectra exhibited slightly more fluctuation compared to that of the specular reflectance spectra. The classification accuracy values for the SVM model for each wood species are summarized in Table 4.

Table 3. Classification Correctness of Specular and Diffuse Reflectance Spectra Under Different Classifiers

	SVM	KNN	CNN	DT	NCM
Specular reflectance spectrum	88.43%	80.00%	64.48%	72.19%	56.97%
Diffuse reflectance spectrum	88.02%	76.56%	62.81%	65.10%	48.33%

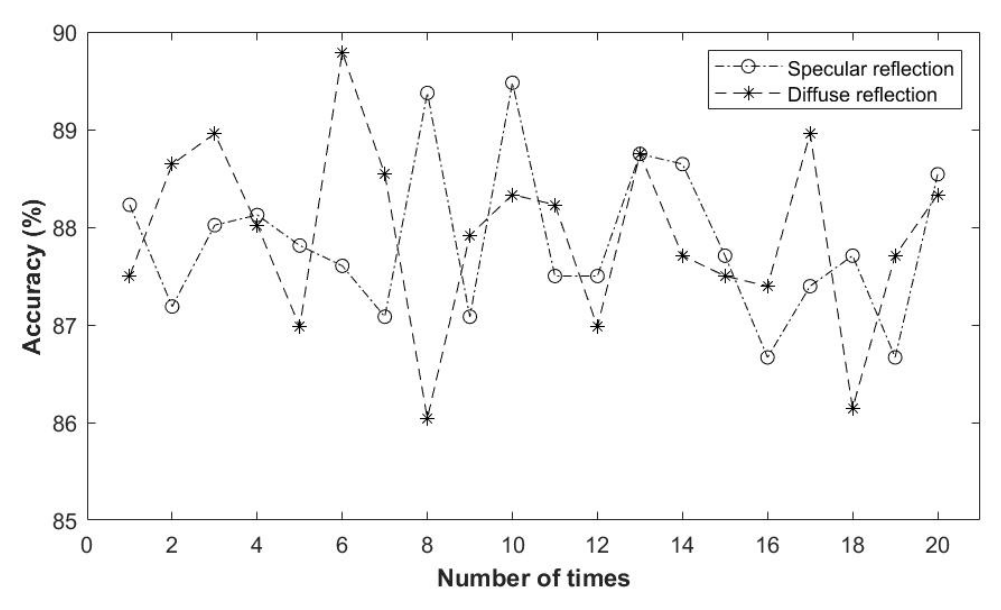


Fig. 6. Classification results of SVM classifier for two types of spectra for 20 training and testing cases

Serial number	1	2	3	4	5	6	7	8
Specular	100%	86.67%	100%	100%	100%	93.33%	100%	93.33%
Diffuse	100%	93.33%	100%	100%	66.67%	93.33%	93.33%	66.67%
Serial number	9	10	11	12	13	14	15	16
Specular	86.67%	86.67%	100%	60%	100%	66.67%	93.33%	93.33%
Diffuse	80%	73.33%	93.33%	100%	93.33%	80%	86.67%	100%
Serial number	17	18	19	20	21	22	23	24
Specular	100%	86.67%	33.33%	80%	100%	80%	73.33%	60%
Diffuse	80%	93.33%	73.33%	80%	100%	93.33%	73.33%	80%
Serial number	25	26	27	28	29	30	31	32
Specular	80%	86.67%	86.67%	86.67%	66.67%	93.33%	86.67%	100%
Diffuse	86.67%	66.67%	93.33%	100%	100%	80%	93.33%	100%
Serial number	33	34	35	36	37	38	39	40
Specular	73.33%	100%	86.67%	86.67%	93.33%	86.67%	100%	86.67%
Diffuse	93.33%	93.33%	60%	93.33%	80%	80%	73.33%	66.67%
Serial number	41	42	43	44	45	46	47	48
Specular	100%	100%	86.67%	100%	93.33%	93.33%	80%	86.67%
Diffuse	100%	100%	53.33%	80%	100%	93.33%	86.67%	93.33%
Serial number	49	50	51	52	53	54	55	56
Specular	80%	40%	100%	80%	40%	93.33%	80%	100%
Diffuse	86.67%	60%	100%	73.33%	86.67%	100%	93.33%	93.33%
Serial number	57	58	59	60	61	62	63	64
Specular	100%	100%	86.67%	100%	100%	93.33%	100%	100%
Diffuse	93.33%	93.33%	93.33%	100%	33.33%	66.67%	100%	80%

Table 4. Correct Classification Rate for Each Wood Species under the SVM Classifier

Among the 64 wood species, 23 species in the specular reflectance spectra and 16 species in the diffuse reflectance spectra achieved 100% classification accuracy. In the specular reflectance spectra, species 19, 50, and 53 exhibited lower classification accuracy. A common characteristic of these species is the distinct color variation bands in the cross sections of the wood samples, as illustrated in (Fig. 7). In the diffuse reflectance spectra, species 35, 43, and 61 exhibited lower classification accuracy. These species can be grouped into two categories—that is, species with considerable variation in black tubular holes in the cross section (such as species 35 and 43), species with more uniform color in the cross section, and less distinct grain features (such as species 61). Figure 7 illustrates the schematic cross sections of these wood species.



Fig. 7. Schematic cross sections of wood species with low correct classification in specular and diffuse reflectance spectra

Additionally, three tree species were classified with an accuracy of less than 50% in the specular reflectance spectrum, whereas only one species had an accuracy of less than 50% in the diffuse reflectance spectrum. In other words, although the overall classification accuracy of the specular reflectance spectrum was slightly higher than that of the diffuse reflectance spectrum, the accuracy was lower for species with distinct color bands in wood sample cross sections. In contrast, the diffuse reflectance spectrum exhibited a more stable classification performance, with fewer species exhibiting low classification accuracy.

Next, the classification accuracy of the NIR spectra across different wavelength bands was explored. From Fig. 5 it is evident that the spectral reflectance curves of the cross sections of the wood samples exhibited more complex waveform changes within the 1200 to 1500 nm range, whereas they remained smoother in other wavelength ranges. Consequently, the entire spectral reflectance curve could be divided into three bands—that is, the 939 to 1181, 1186 to 1423, and 1428 to 1671 nm bands. Table 5 presents the classification accuracies of different classifiers for these wavelength bands. From Table 5, it is evident that the classification performance of the SVM classifier in the two end bands was inferior to that in the middle band. Additionally, after segmenting the entire spectral band into three parts, the classification accuracy decreased compared with that of the original unsegmented band. All classifiers, except the SVM, exhibited higher classification accuracy for the specular reflectance spectrum than for the diffuse reflectance spectrum across different bands.

It is worth noting that the CNN classifier was not included in Table 5 because each segmented band contained only 42 dimensions. Following feature extraction using a CNN, the feature dimensions were reduced to only two, limiting its utility in this context.

Table 5. Comparison of Classification Accuracies of Specular and Diffuse Reflectance Spectra Across Different Wavelength Bands

Model	Specular Reflection					
	939 to 1181 nm	1186 to 1423 nm	1428 to 1671 nm			
SVM	74.24%	74.75%	65.00%			
KNN	72.71%	40.31%	74.17%			
DT	53.90%	48.70%	45.00%			
NCM	49.48%	42.81%	42.92%			
Model		Diffuse Reflection				
	939 to 1181 nm	1186 to 1423 nm	1428 to 1671 nm			
SVM	69.34%	81.18%	67.22%			
KNN	67.60%	34.69%	72.08%			
DT	48.30%	43.50%	35.30%			
NCM	44.90%	34.79%	34.79%			

Cross Use of Classifier Models Trained with Two Types of Spectra

This section discusses the feasibility of cross-using classifier models trained with specular and diffuse reflectance spectra, with the specific classification results provided in Table 6. It is evident that neither the classifier model trained with specular reflectance spectra, nor the model trained with diffuse reflectance spectra can be used interchangeably. In terms of classification accuracy, the NCM classifier performed slightly better than the other classifiers; however, all the classifiers exhibited accuracies below 16%. This was due to the sensitivity of the spectral reflectance curve to the surface properties of the object. Although the specular and diffuse reflectance spectra exhibited similar trends (mathematically expressible as differentials), differences in their values led to considerably lower classification accuracy when the classifiers were cross used. Consequently, when collecting spectral profiles of wood cross sections, it is essential to distinguish between diffuse and specular reflectance spectra. The classifier models generated by training each type cannot be used interchangeably.

Table 6. Comparison of Classification Accuracies After Cross Use of Classifier Models for the Two Spectral Classes

Classifier Models Trained on Specular Reflection Spectrum								
Classifier model	Classifier model SVM KNN CNN DT NCM							
Diffuse reflection	12.08%	13.65%	12.80%	11.25%	15.94%			
Classifier Model Trained on Diffuse Reflectance Spectrum								
Classifier model	SVM	KNN	CNN	DT	NCM			
Specular reflection	13.12%	13.54%	11.40%	8.20%	12.08%			

CONCLUSIONS

In this study, the characteristics of the specular and diffuse reflectance spectra from the cross sections of timber samples were examined, along with a comparison of their classification performance in identifying timber species using NIR spectra. A total of 64 experimental timber samples were used. The following conclusions were drawn:

- 1. The specular reflectance spectra generally exhibited superior classification performance compared to the diffuse reflectance spectra, as confirmed by the evaluation metrics based on the intraclass and interclass scatter matrices. Consequently, it is recommended that the specular reflection NIR spectral profile should be selected as a feature for classifying and identifying timber species.
- 2. Among the tested classifiers, the SVM classifier demonstrated the highest classification accuracy, with both types of spectra achieving similarly high classification rates. This can be attributed to the fact that SVMs use a combination of binary classifiers for multiclass classification, employing three strategies—that is, 1-vs-1, 1-vs-rest, and one-class SVM. The effective combination of these binary classifiers enhances the generalization ability of the SVM model. Moreover, the SVM model uses kernel functions to map samples that are challenging to classify in a low-dimensional space into a higher-dimensional space, thereby facilitating a more effective classification. These advantages enable the SVM classifier to overcome the inherent distributional differences between the two types of spectra, resulting in consistently high classification accuracy.
- 3. In contrast, the generalized classification performance of the other classifiers was limited, and their accuracy was heavily influenced by the separability of the patterns within the two types of spectra. Consequently, these classifiers also performed better on the specular reflectance spectra than on the diffuse reflectance spectra.
- 4. The classifier models trained on the specular and diffuse reflection spectra were found to be non-interchangeable, indicating that the models developed for one type of spectrum could not be substituted for the other.

ACKNOWLEDGMENTS

This study was supported by the following grants, which are gratefully acknowledged. National Natural Science Foundation of China (Grant number 62265001), and the Guangxi University of Science and Technology Doctoral Research Fund (Grant number 22Z07).

Availability of Data and Materials

The wood spectral dataset used in this work is confidential, but this dataset used to support the findings of this study is available from the corresponding author upon request after this article is accepted and published online.

Competing Interests

The authors declare that they have no competing interests.

Author Contributions

Peng Zhao proposed the research idea and the experimental framework, writing the whole manuscript. Cheng-Kun Wang carried out the wood species recognition comparative experiments and collated the experimental results. Li-Na Dong and Mao-Ni Zhao collated the experimental results. All authors read and approved the final manuscript.

REFERENCES CITED

- Antil, S., Abraham, J. S., Sripoorna, S., Maurya, S., Dagar, J., Makhija, S., Bhagat, P., Gupta, R., Sood, U., and Lal, R. (2023). "DNA barcoding, an effective tool for species identification: a review," *Molecular Biology Reports* 50(1), 761-775. DOI: 10.1007/s11033-022-08015-7
- Deklerck, V., Lancaster, C. A., Van Acker, J., Espinoza, E. O., Van den Bulcke, J., and Beeckman, H. (2020). "Chemical fingerprinting of wood sampled along a pith-to-bark gradient for individual comparison and provenance identification," *Forests* 11(1), article 107. DOI: 10.3390/f11010107
- Hearst, M. A., Dumais, S. T., Osuna, E., Platt, J., and Scholkopf, B. (1998). "Support vector machines," *IEEE Intelligent Systems and their applications* 13(4), 18-28. DOI: 10.1109/5254.708428
- Kanayama, H., Ma, T., Tsuchikawa, S., and Inagaki, T. (2019). "Cognitive spectroscopy for wood species identification: near infrared hyperspectral imaging combined with convolutional neural networks," *Analyst* 144(21), 6438-6446. DOI: 10.1039/C9AN01180C
- Luo, L., Xu, Z. J., and Na, B. (2023). "Building machine learning models to identify wood species based on near-infrared spectroscopy," *Holzforschung* 77(5), 326-337. DOI: 10.1515/hf-2022-0122
- Ma, T., Inagaki, T., Ban, M., and Tsuchikawa, S. (2019). "Rapid identification of wood species by near-infrared spatially resolved spectroscopy (NIR-SRS) based on hyperspectral imaging (HSI)," *Holzforschung* 73(4), 323-330. DOI: 10.1515/hf-2018-0128

- Pan, X., Qiu, J., and Yang, Z. (2023). "Identification of softwood species using convolutional neural networks and raw near-infrared spectroscopy," *Wood Material Science & Engineering* 18(4), 1338-1348. DOI: 10.1080/17480272.2022.2130822
- Peterson, L. E. (2009). "K-nearest neighbor," *Scholarpedia* 4(2), article 1883. DOI: 10.4249/scholarpedia.1883
- Safavian, S. R., and Landgrebe, D. (1991). "A survey of decision tree classifier methodology," *IEEE Transactions on Systems, Man, and Cybernetics* 21(3), 660-674. DOI: 10.1109/21.97458
- Sharma, V., Yadav, J., Kumar, R., Tesarova, D., Ekielski, A., and Mishra, P. K. (2020). "On the rapid and non-destructive approach for wood identification using ATR-FTIR spectroscopy and chemometric methods," *Vibrational Spectroscopy* 110, article ID 103097. DOI: 10.1016/j.vibspec.2020.103097
- Veenman, C. J., and Reinders, M. J. T. (2005). "The nearest subclass classifier: A compromise between the nearest mean and nearest neighbor classifier," *IEEE Transactions on Pattern Analysis and Machine Intelligence* 27(9), 1417-1429. DOI: 10.1109/TPAMI.2005.187
- Verly Lopes, D. J., Burgreen, G. W., and Entsminger, E. D. (2020). "North American hardwoods identification using machine-learning," *Forests* 11(3), article 298. DOI: 10.3390/f11030298
- Wang, C. K., Zhao, P., and Yang, J. L. (2024). "Effect of wood surface finish on wood species classification using spectral reflectance," *BioResources* 19(2), 3060-3077. DOI: 10.15376/biores.19.2.3060-3077
- Zhan, W., Chen, B., Wu, X., Yang, Z., Lin, C., Lin, J., and Guan, X. (2023). "Wood identification of *Cyclobalanopsis* (Endl.) Oerst based on microscopic features and CTGAN-enhanced explainable machine learning models," *Frontiers in Plant Science* 14, article ID 1203836. DOI: 10.3389/fpls.2023.1203836
- Zhang, M., Xie, X., Zhang, D., Chen, R., Xu, Y., Wang, J., Liu, J., and Xu, X. (2023). "Nondestructive identification of wood species by terahertz spectrum," *Microwave and Optical Technology Letters* 65(5), 1117-1121. DOI: 10.1002/mop.33195

Article submitted: December 31, 2024; Peer review completed: February 1, 2025; Revised version received: February 12, 2025; Accepted: February 28, 2025; Published: June 24, 2025.

DOI: 10.15376/biores.20.3.6648-6661